

Core-excitation effects in $^{20}\text{O}(d, p)^{21}\text{O}$ transfer reactions: Suppression or enhancement?

A. Deltuva, D. Jurčiukonis, E. Norvaišas

Institute of Theoretical Physics and Astronomy, Vilnius University, Saulėtekio al. 3, LT-10222 Vilnius, Lithuania

Abstract

$^{20}\text{O}(d, p)^{21}\text{O}$ transfer reactions are described using momentum-space Faddeev-type equations for transition operators and including the vibrational excitation of the ^{20}O core. The available experimental cross section data at 10.5 MeV/nucleon beam energy for the ^{21}O ground state $\frac{5}{2}^+$ and excited state $\frac{1}{2}^+$ are quite well reproduced by our calculations including the core excitation. Its effect can be roughly simulated reducing the single-particle cross section by the corresponding spectroscopic factor. Consequently, the extraction of the spectroscopic factors taking the ratio of experimental data and single-particle cross section at this energy is a reasonable procedure. However, at higher energies core-excitation effects are much more complicated and have no simple relation to spectroscopic factors. We found that core-excitation effects are qualitatively very different for reactions with the orbital angular momentum transfer $\ell = 0$ and $\ell = 2$, suppressing the cross sections for the former and enhancing for the latter, and changes the shape of the angular distribution in both cases. Furthermore, the core-excitation effect is a result of a complicated interplay between its contributions of the two- and three-body nature.

Key words: Three-body scattering, core excitation, transfer reactions, spectroscopic factor

PACS: 24.10.-i, 21.45.-v, 25.45.Hi, 25.40.Hs

1. Introduction

Interactions between nucleons (N) and composite nuclei (A) are usually modeled by two-body effective optical or binding potentials acting between structureless particles. This scheme works quite well for stable tightly bound nuclei but may become a poor approximation for exotic nuclei that nowadays are extensively studied both experimentally and theoretically. An improvement of the structureless nucleus model, at a first step, consists in explicitly considering also its lowest excited states (A^*), thereby accounting for the compositeness of the nucleus A in an approximate way. This extension has been proposed long ago [1] and applied to numerous studies of elastic and inelastic $N + A$ scattering. However, the application of interaction models including the excitation of the involved nucleus, also called the core excitation, to three-body nuclear reactions, e.g., deuteron (d) stripping and pickup, is still a complicated task. First studies of (d, p) reactions demonstrating the importance of the core exci-

tation [2–5] were based on two-body-like approaches such as the distorted-wave Born approximation (DWBA) and coupled-channels Born approximation (CCBA) that relied on deuteron-nucleus optical potentials. Only quite recently the three-body calculations have emerged that include the core excitation. Extensions of the DWBA [6,7] and continuum discretized coupled channels (CDCC) method [8,9] mostly focused on the breakup reactions, in particular, of ^{11}Be . The calculations for neutron transfer reactions $^{10}\text{Be}(d, p)^{11}\text{Be}$ and $^{11}\text{Be}(p, d)^{10}\text{Be}$ were performed using rigorous Faddeev three-body scattering theory [10] in the form of Alt, Grassberger, and Sandhas (AGS) equations [11] for transition operators, solved in the extended Hilbert space [12–14]. The latter works demonstrated that in the deuteron stripping and pickup the core excitation effect cannot be simply simulated by the reduction of the cross section according to the respective spectroscopic factor (SF). It was found that extracting the SF from the ratio of experimental and theoretical transfer cross sections, as often used with the adiabatic distorted wave approximation (ADWA) calculations [15], may lead to a strong underestimation of the SF. Calculations of Refs. [12–14] employed the rotational model [1] for the excitation of the ^{10}Be core;

Email addresses: arnoldas.deltuva@tfai.vu.lt (A. Deltuva),
darius.jurciukonis@tfai.vu.lt (D. Jurčiukonis),
egidijus.norvaisas@tfai.vu.lt (E. Norvaišas).

the most prominent core-excitation effects have been observed for the $^{10}\text{Be}(d,p)^{11}\text{Be}$ transfer to the ground state of $^{11}\text{Be}(\frac{1}{2}^+)$ whose dominant component corresponds to an S -wave neutron coupled to the $^{10}\text{Be}(0^+)$ ground state, i.e., the orbital angular momentum transfer for this reaction is $\ell = 0$. In contrast, for the $\ell = 1$ transfer leading to the excited state $^{11}\text{Be}(\frac{1}{2}^-)$ the core-excitation effects have been less remarkable. It is therefore very important to clarify the systematics of the core-excitation effects in transfer reactions, investigating other types of excitation mechanisms and bound states. Furthermore, a deeper understanding may be gained by disentangling the effects of two- and three-body nature. The study of $^{20}\text{O}(d,p)^{21}\text{O}$ transfer reactions intended in the present work leads to the desired goal and is interesting for several reasons. First, the $^{21}\text{O}(\frac{5}{2}^+)$ ground state has a significant component of D -wave neutron coupled to the $^{20}\text{O}(0^+)$ ground state, thereby allowing the extension of systematics from Refs. [12–14] to the D -wave neutron state and $\ell = 2$ transfer. Second, the lowest excitation of the ^{20}O core 2^+ has a vibrational character, giving opportunity to investigate the vibrational model for the nucleon-core interaction [1] in the context of transfer reactions. Last but not least there are experimental data for $^{20}\text{O}(d,p)^{21}\text{O}$ transfer reactions at 10.5 MeV/nucleon beam energy [16] that have not yet been analyzed with rigorous Faddeev-type calculations.

In Sec. 2 we shortly recall the three-body scattering equations with core excitation, and in Sec. 3 describe the employed nucleon- ^{20}O potentials. Results are presented in Sec. 4, and a summary is given in Sec. 5.

2. Solution of three-body scattering equations with core excitation

The numerical technique for calculating deuteron-nucleus reactions with the inclusion of the core excitation is taken over from Refs. [12–14] but further developments are needed to get insight into separate core-excitation contributions of the two- and three-body nature. The method is based on the integral formulation of rigorous Faddeev-type three-body scattering theory for transition operators as proposed by Alt, Grassberger, and Sandhas [11], but extended for the Hilbert space $\mathcal{H}_g \oplus \mathcal{H}_x$ whose sectors correspond to the core being in its ground (g) or excited (x) state. These sectors are coupled by the nucleon-core two-body potentials v_α^{ji} where the superscripts j and i , being either g or x , label the internal states of the core, and the subscript α , being A , p , or n , labels the spectator particle in the odd-man-out notation. Consequently, the respective two-body transition operators

$$T_\alpha^{ki} = v_\alpha^{ki} + \sum_{j=g,x} v_\alpha^{kj} G_0^j T_\alpha^{ji} \quad (1)$$

and three-body transition operators

$$U_{\beta\alpha}^{ki} = \bar{\delta}_{\beta\alpha} \delta_{ki} G_0^{i-1} + \sum_{\gamma=A,p,n} \sum_{j=g,x} \bar{\delta}_{\beta\gamma} T_\gamma^{kj} G_0^j U_{\gamma\alpha}^{ji} \quad (2)$$

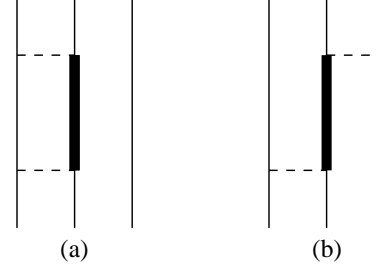


Fig. 1. Diagrammatic representation of the lowest-order core-excitation contributions of (a) two-body and (b) three-body nature. Horizontal dashed lines stand for potentials while vertical solid lines stand for particles, the thick one being for the core in its excited state.

couple \mathcal{H}_g and \mathcal{H}_x as well. Here $\bar{\delta}_{\beta\alpha} = 1 - \delta_{\beta\alpha}$ and $G_0^j = (E + i0 - \delta_{jx} \Delta m_A - K)^{-1}$ is the projection of the free resolvent into \mathcal{H}_j , with E , Δm_A , and K being the available energy in the center-of-mass (c.m.) frame, core-excitation energy, and kinetic energy operator, respectively. The amplitudes for deuteron stripping reactions $A(d,p)B$, B denoting the (An) bound state, are given by the on-shell matrix elements $\langle \Phi_p^g | U_{pA}^{gg} | \Phi_A^g \rangle + \langle \Phi_p^x | U_{pA}^{xg} | \Phi_A^g \rangle$ since the final $p + B$ channel state $|\Phi_p\rangle = |\Phi_p^g\rangle + |\Phi_p^x\rangle$ has components in both Hilbert sectors.

The core-excitation effects can be separated into contributions of two- and three-body nature. The former consists in modifying T_α^{gg} through intermediate core excitations, i.e., through the terms of type $v_\alpha^{gx} G_0^x v_\alpha^{xg}$ and so on in the iterated coupled-channel Lippmann-Schwinger equation (1). The contribution of the three-body nature arises due to nondiagonal components T_α^{xg} and T_α^{gx} that are responsible for the coupling of the two Hilbert sectors in Eq. (2), i.e., $T_\beta^{gx} \bar{\delta}_{\beta\alpha} G_0^x T_\alpha^{xg}$ and so on, yielding, in fact, an energy-dependent effective three-body force (E3BF). Lowest-order diagrams for both types are depicted in Fig. 1. We note a formal similarity between these contributions and the so-called dispersive and three-nucleon force effects arising in the description of the three-nucleon system with the Δ -isobar excitation [17,18]. Since the full core-excitation effect will be extracted from the solution of Eq. (2), to get insight into the importance of separate two- and three-body contributions it is enough to exclude one of them. It is most convenient to do so for the E3BF, whose exclusion can be achieved by setting $T_\gamma^{kj} = \delta_{kj} \delta_{jg} T_\gamma^{gg}$ in Eq. (2). This type of results will be labeled in the following as “no E3BF”.

Although the present work employs the potentials v_α^{ji} derived from the vibrational model [1], calculations proceed in the same way as with rotational model potentials used in Refs. [12–14]. The AGS equations (2) are solved numerically in the momentum-space partial-wave representation. Six sets of base functions $|p_\alpha q_\alpha(l_\alpha\{[L_\alpha(s_\beta^i s_\gamma^i) S_\alpha^i] j_\alpha^i s_\alpha^i\} \mathcal{S}_\alpha^i) JM\rangle$ are employed with $(\alpha\beta\gamma) = (Apn)$, (pnA) , or (nAp) , and $i = g$ or x . Here p_α and q_α are magnitudes of Jacobi momenta for the configuration $\alpha(\beta\gamma)$ while L_α and l_α are the associated orbital angular momenta. Furthermore, s_A^i and $s_p^i = s_n^i = \frac{1}{2}$ are

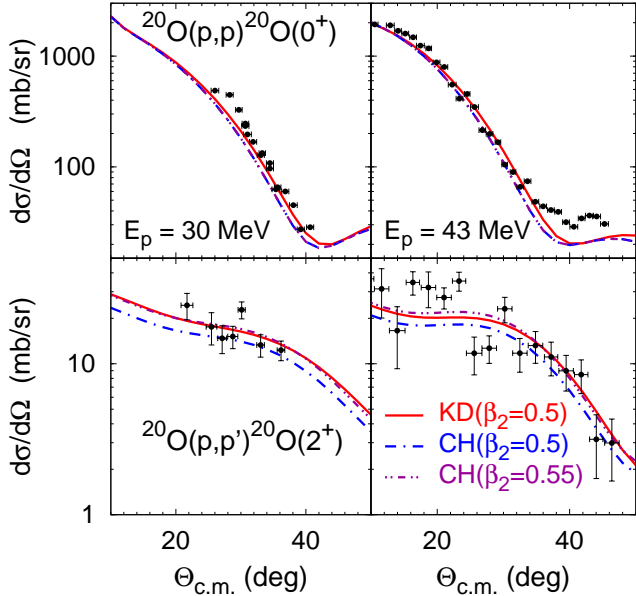


Fig. 2. (Color online) Differential cross sections $d\sigma/d\Omega$ for elastic (top) and inelastic (bottom) $p+^{20}\text{O}$ scattering at 30 (left) and 43 (right) MeV/nucleon beam energies as functions of the c.m. scattering angle $\Theta_{\text{c.m.}}$. Results including the core excitation based on KD and CH potential models with $\beta_2 = 0.5$ and 0.55 are compared with the experimental data from Ref. [22] (30 MeV) and Ref. [23] (43 MeV).

spins of the corresponding particles, among them only s_A^i depends on the Hilbert sector i , i.e., $s_A^g = 0$ and $s_A^x = 2$ in the considered case of the ^{20}O nucleus with the ground and first excited states 0^+ and 2^+ , respectively. All discrete angular momentum quantum numbers, via the intermediate angular momenta S_α^i , j_α^i , and S_α^i , are coupled to the total angular momentum J with the projection M . We note that the spin $s_A^x = 2$ implies roughly five times more basis states in \mathcal{H}_x as compared to \mathcal{H}_g , thereby increasing the demand on computer memory and time by a factor of 20 to 40. Including more states of the core, e.g., the second excited state 4^+ would be even significantly more demanding, and for this reason we restrict our present calculations to the inclusion of 0^+ and 2^+ states of ^{20}O . Well-converged results for $^{20}\text{O}(d,p)^{21}\text{O}$ transfer reactions are obtained by including $J \leq 25$ states with $L_A \leq 3$, $L_p \leq 5$, and $L_n \leq 10$. Higher value for L_n is needed due to the Coulomb force present within the $A+p$ pair which is included via the screening and renormalization method [19–21].

3. Potentials

We consider the system of a proton, a neutron, and a ^{20}O core with masses $m_p = 0.99931 m_N$, $m_n = 1.00069 m_N$, and $m_A = 19.84153 m_N$ given in units of $m_N = (m_n + m_p)/2 = 938.919$ MeV; the core excitation energy is $\Delta m_A = 1.684$ MeV. To the best of our knowledge, potentials specifically designed for the $N+^{20}\text{O}$ interaction including the core excitation are not available. The corresponding experimental data are scarce, we are

aware of only two $p+^{20}\text{O}$ elastic and inelastic scattering measurements at 30 [22] and 43 [23] MeV/nucleon beam energies. In these works the data have been analyzed using DWBA or coupled-channel calculations with global optical potentials, e.g., [24]. Extracted values of the quadrupole vibrational coupling parameter β_2 are 0.50 ± 0.04 [22] and 0.55 ± 0.06 [23]. We also base our calculations on global optical potentials but use more modern parametrizations, namely, those of Koning-Delaroche (KD) [25] and Chapel Hill 89 (CH) [26]. These potentials were designed for $A \geq 24$ and $A \geq 40$ nuclei, respectively, but one may expect a reasonable extrapolation also to $A = 20$, especially for the KD potential. To include the core excitation, we extended these potentials for quadrupole vibrations [1] and modify by the subtraction method of Ref. [13] adding a nonlocal contribution. The terms up to the second order in β_2 as given in Ref. [1] are taken into account in our calculations. It turns out that such an approach reproduces the experimental data for elastic and inelastic differential cross sections of Refs. [22,23] reasonably well using the same value $\beta_2 = 0.5$ as shown in Fig. 2, especially for the KD potential. To study the sensitivity to β_2 , we also show CH predictions with $\beta_2 = 0.55$, that yield a better description of the inelastic cross section. The observed agreement encourages the application of these potentials for $^{20}\text{O}(d,p)^{21}\text{O}$ transfer reactions, not only for $p+^{20}\text{O}$ but also for $n+^{20}\text{O}$ pair where no experimental scattering data are available. An exception is the $n+^{20}\text{O}$ potential in the $\frac{5}{2}^+$ and $\frac{1}{2}^+$ partial waves that must be real to support bound states with the binding energies of 3.806 and 2.586 MeV, respectively. In addition, predictions of various shell models [27,28] for SF's of these states are available, being around 0.33 to 0.34 for $\frac{5}{2}^+$ and 0.81 to 0.83 for $\frac{1}{2}^+$ [16]. We include this information in constraining the $n+^{20}\text{O}$ potentials. We start with the undeformed coordinate-space potential

$$v_\alpha(r) = -V_c f(r, R, a) + \mathbf{L}^2 V_L f(r, R, a) + \boldsymbol{\sigma} \cdot \mathbf{L} V_{so} \frac{2}{r} \frac{d}{dr} f(r, R, a), \quad (3)$$

where $f(r, R, a) = [1 + \exp((r - R)/a)]^{-1}$ is Woods-Saxon form factor, $a = 0.65$ fm, $V_{so} = 6.0$ MeV \cdot fm², and R is taken from the real part of the optical potential acting in other waves, i.e., $R = 3.13$ fm (3.17 fm) for KD (CH) potentials. In addition to standard central and spin-orbit terms a phenomenological \mathbf{L}^2 term is taken over from Ref. [29]. The core excitation is included by quadrupole vibrations of the central part in (3) with $\beta_2 = 0.5$ or 0.55 as described by Tamura [1]. Potential strength parameters V_c and V_L are adjusted to reproduce the desired binding energies and SF's. The latter are chosen to be the middle values of several shell model predictions [16], i.e., 0.34 for $\frac{5}{2}^+$ and 0.82 for $\frac{1}{2}^+$. Deeply-bound Pauli forbidden states are projected out. The resulting potential parameters are collected in Tables 1 and 2; parameter sets with $\beta_2 = 0.0$ correspond to single-particle models without core excitation that are used to isolate its effect.

Table 1

Quadrupole vibration parameter β_2 , Woods-Saxon radius R , potential strengths V_c and V_L , and the resulting SF for the ^{21}O ground state $\frac{5}{2}^+$ with the binding energy of 3.806 MeV.

β_2	$R(\text{fm})$	$V_c(\text{MeV})$	V_L/V_c	SF
0.50	3.13	53.564	0.0389	0.34
0.50	3.17	52.580	0.0396	0.34
0.55	3.17	51.907	0.0419	0.34
0.0	3.19	50.425	0.0	1.0
0.0	3.23	49.347	0.0	1.0

Table 2

Quadrupole vibration parameter β_2 , Woods-Saxon radius R , potential strengths V_c and V_L , and the resulting SF for the ^{21}O excited state $\frac{1}{2}^+$ with the binding energy of 2.586 MeV.

β_2	$R(\text{fm})$	$V_c(\text{MeV})$	V_L/V_c	SF
0.50	3.13	45.531	0.0252	0.82
0.50	3.17	44.639	0.0260	0.82
0.55	3.17	44.038	0.0308	0.82
0.0	3.19	49.743	0.0	1.0
0.0	3.23	48.813	0.0	1.0

4. Results

Taking $p+^{20}\text{O}$ and $n+^{20}\text{O}$ potentials from previous section together with the high-precision charge-dependent (CD) Bonn $n+p$ potential [30] as the dynamic input, we solve the AGS equations (2) and calculate $^{20}\text{O}(d,p)^{21}\text{O}$ differential cross sections $d\sigma/d\Omega$ as functions of the c.m. scattering angle $\Theta_{\text{c.m.}}$. We start with 10.5 MeV/nucleon beam energy, corresponding to the deuteron beam energy $E_d = 21$ MeV, where the experimental data [16] are available. The results obtained without ($\beta_2 = 0$) and with ($\beta_2 = 0.5$) core excitation based on KD and CH potentials are presented in Fig. 3. The core excitation effect for the transfer to the ^{21}O ground state $\frac{5}{2}^+$ is very large. It strongly reduces the differential cross section bringing it in a good agreement with the experimental data. The sensitivity to the potential model is visible except at very small angles but remains smaller than experimental error bars. To study the sensitivity to β_2 we include also CH-based predictions with $\beta_2 = 0.55$; they are almost indistinguishable from the corresponding $\beta_2 = 0.5$ results, indicating that the value of β_2 is not critical for transfer observables provided that other properties are fixed. Same conclusions regarding the sensitivity to β_2 and potential apply also for the transfer to the ^{21}O excited state $\frac{1}{2}^+$. However, in this case the core excitation effect is smaller, although it also reduces the differential cross section bringing it closer to the data, except for few points at larger angles. There is also some mismatch between predicted and measured positions of the minimum. We note that for both reactions KD predictions are slightly higher, possibly due to a larger elastic $N+^{20}\text{O}$ cross section.

Obviously, the reduction of the differential cross section

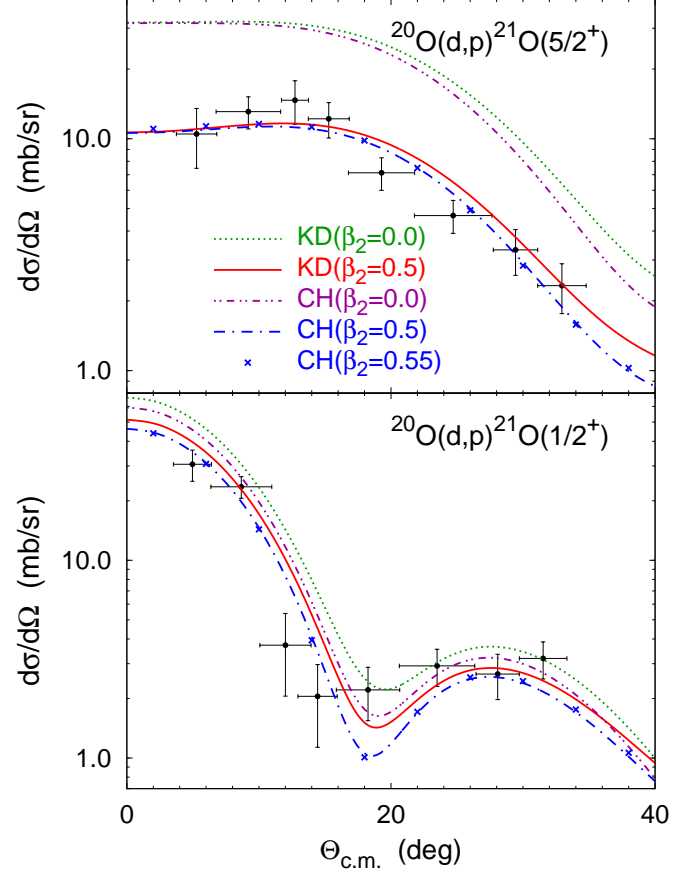


Fig. 3. (Color online) Differential cross section for $^{20}\text{O}(d,p)^{21}\text{O}$ transfer reactions at $E_d = 21$ MeV leading to ^{21}O ground $\frac{5}{2}^+$ (top) and excited $\frac{1}{2}^+$ (bottom) states. Predictions obtained with and without the vibrational core excitation based on KD and CH potential models are compared with the experimental data from Ref. [16].

due to the core excitation correlates with the reduction of the SF from unity to 0.34 and 0.82 for ground and excited states, respectively. In naive reaction methods like DWBA or ADWA the dynamic core excitation is usually neglected, i.e., it is assumed that the bound state component $|\Phi_p^x\rangle$ takes no part in the reaction, and the core excitation effect is a reduction of the single-particle differential cross section by the SF. However, this conjecture on factorization may be wrong as it was demonstrated by rigorous Faddeev-type calculations using the $^{10}\text{Be}(d,p)^{11}\text{Be}$ transfer to the ground state of $^{11}\text{Be}(\frac{1}{2}^+)$ as example [12–14]. We therefore investigate in Figs. 4 and 5 the validity of factorization conjecture for $^{20}\text{O}(d,p)^{21}\text{O}$ reactions over a broader energy range. Having no more experimental data, we simply take additional energy value larger by a factor of 3, i.e., $E_d = 63$ MeV. As the core excitation effects for KD and CH turn out to be quite similar, we show only KD results that in general are closer to the experimental two- and three-body data. We multiply KD single-particle $\beta_2 = 0$ differential cross sections by the respective SF of the model with the core excitation and compare with the KD($\beta_2 = 0.5$) results fully including the core excitation. The difference between these two results, or the deviation of the ratio

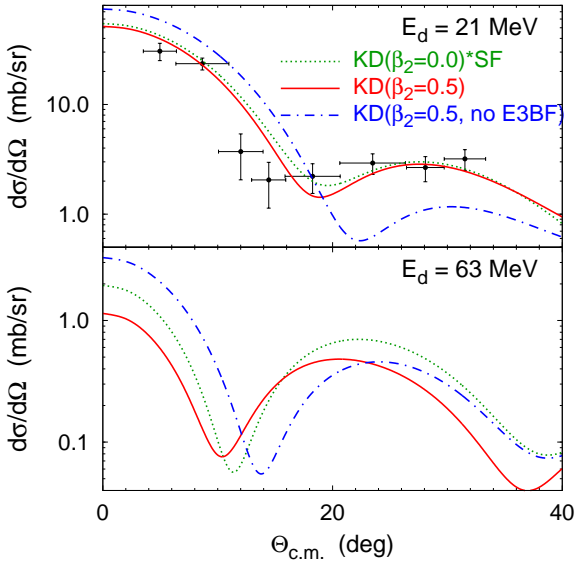


Fig. 4. (Color online) Differential cross section for $^{20}\text{O}(d,p)^{21}\text{O}$ transfer reactions at $E_d = 21$ and 63 MeV leading to ^{21}O excited $\frac{1}{2}^+$ state. Single-particle predictions scaled by $\text{SF} = 0.82$ (dotted curves) are compared with results including the core excitation in full (solid curves) and excluding the E3BF contribution (dash-dotted curves). The experimental data at $E_d = 21$ MeV are from Ref. [16].

$$R_x = \frac{d\sigma/d\Omega(\beta_2 = 0.5)}{\text{SF} \cdot d\sigma/d\Omega(\beta_2 = 0)} \quad (4)$$

from unity indicates violation of the factorization conjecture. We start with the excited state $\frac{1}{2}^+$ analysis in Fig. 4 where we expect some similarities with the $^{11}\text{Be}(\frac{1}{2}^+)$ case [12–14]. At $E_d = 21$ MeV the two curves are close but, at least below the first minimum, differ by a roughly constant factor, i.e., the core excitation effect is slightly, by about 6%, stronger than predicted by the factorization conjecture. Having the SF of 0.82 the core excitation reduces the differential cross section at forward angles by a factor of 0.77 which is exactly the value of the SF extracted in Ref. [16] relying on the factorization conjecture. Thus, the dynamical core excitation model well explains a stronger reduction of the cross section observed in Ref. [16] as compared to the factorization conjecture. The deviation between the two curves in Fig. 4 increases with increasing energy, and their ratio becomes angle-dependent, thereby indicating that the factorization conjecture fails at higher energies. The reduction of the cross section at forward angles is significantly stronger than SF, e.g., $R_x = 0.59$ at $E_d = 63$ MeV and $\Theta_{\text{c.m.}} = 0^\circ$. Such a behavior is indeed qualitatively consistent with findings of Refs. [12–14] for $^{11}\text{Be}(\frac{1}{2}^+)$ within the rotational model.

A similar study of the $^{20}\text{O}(d,p)^{21}\text{O}$ transfer to the ^{21}O ground state $\frac{5}{2}^+$ is presented in Fig. 5. At $E_d = 21$ MeV the two curves are again close, especially at forward angles. Thus, despite that $\text{SF} = 0.34$ significantly deviates from unity, the differential cross section including the core excitation scales well with SF, and at this energy the factorization conjecture is valid. However, the situation changes dramatically at higher energy where the two curves deviate

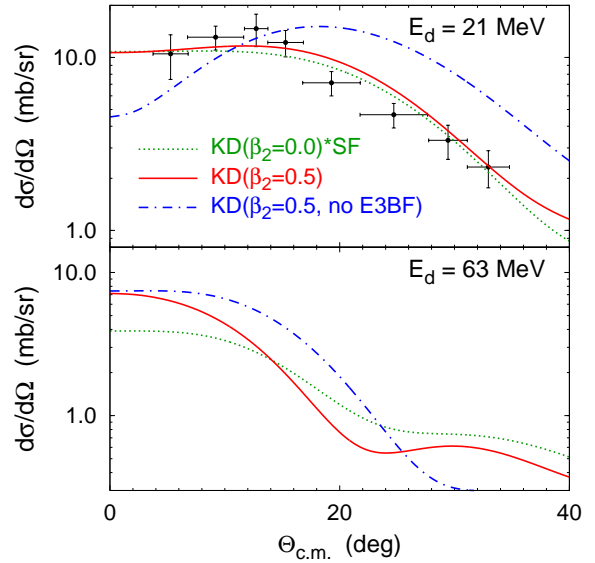


Fig. 5. (Color online) Same as Fig. 4 but for ^{21}O ground state $\frac{5}{2}^+$ with $\text{SF} = 0.34$.

from each other in an angle-dependent way. We emphasize that at forward angles this deviation is in opposite direction as compared to the excited state $\frac{1}{2}^+$, e.g., $R_x = 1.83$ at $E_d = 63$ MeV and $\Theta_{\text{c.m.}} = 0^\circ$. Thus, at higher energies the factorization conjecture fails for the ^{21}O ground state $\frac{5}{2}^+$ as well, but quantitatively the core excitation effect is very different as compared to the one for the excited state $\frac{1}{2}^+$.

In Figs. 4 and 5 we also isolate the E3BF core-excitation effect, given as the difference between the solid and dash-dotted curves. Quite surprisingly, even at $E_d = 21$ MeV it turns out to be significant. Consequently, the core-excitation effect of the two-body nature must be significant as well to cancel the E3BF to a large extent, especially at $E_d = 21$ MeV, such that their sum reproduces the full core-excitation effect. We note that substantial cancellation of the corresponding two- and three-body effects due to the Δ -isobar excitation was often observed also in the nucleon-deuteron scattering [18].

We studied also sensitivity of the transfer cross sections to the neutron-proton tensor force and D -state component in the deuteron. Replacing the CD Bonn potential in the $^3S_1 - ^3D_1$ partial wave by a central one reproducing deuteron binding and, roughly, $n-p$ 3S_1 and 3D_1 phase shifts, leads to small but visible changes (smaller than KD - CH difference) in the cross sections. However, we do not consider such a $n-p$ potential as realistic and therefore performed another test calculation with the realistic Argonne V18 potential [31] that has a stronger tensor force and a larger deuteron D -state probability as compared to CD Bonn. In this case the differences were minor, so we conclude that uncertainties in a realistic $n-p$ force do not affect the $^{20}\text{O}(d,p)^{21}\text{O}$ transfer cross sections.

Finally we consider the deuteron pickup reaction $^{21}\text{O}(p,d)^{20}\text{O}$. For the $d + ^{20}\text{O}(0^+)$ final state it is exactly the time-reverse reaction of $^{20}\text{O}(d,p)^{21}\text{O}$ with the cross sections (at the same c.m. energy) related by the time re-

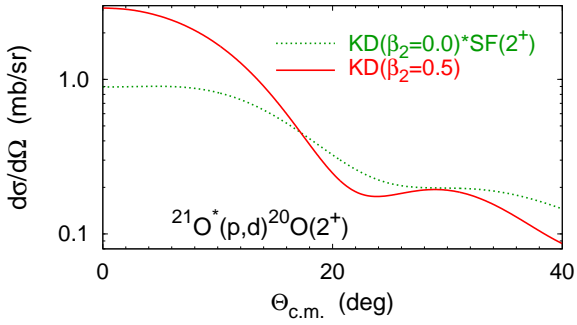


Fig. 6. (Color online) Differential cross section for $^{21}\text{O}^*(p,d)^{20}\text{O}(2^+)$ transfer reactions at $E_p = 60.36$ MeV. Results including the core excitation (solid curve) are compared with single-particle predictions scaled by $\text{SF}(2^+) = 0.18$ (dotted curve).

versal symmetry. In contrast, with the $d + ^{20}\text{O}(2^+)$ final state it presents a new case that we study in Fig. 6 at 60.36 MeV/nucleon beam energy. The initial excited state $^{21}\text{O}(\frac{1}{2}^+)$ this time corresponds to the $\ell = 2$ transfer as the $^{20}\text{O}(2^+)$ component is coupled with a D -wave neutron. The core-excitation effect turns out to be qualitatively similar to another $\ell = 2$ case, i.e., $^{20}\text{O}(d,p)^{21}\text{O}(\frac{5}{2}^+)$ shown in the bottom part of Fig. 5.

5. Summary and conclusions

We analyzed $^{20}\text{O}(d,p)^{21}\text{O}$ transfer reactions taking into account the vibrational excitation of the ^{20}O core. Calculations were performed using Faddeev-type equations for transition operators that were solved in the momentum-space partial-wave representation. Well converged results were obtained for several interaction models based on the vibrational extension of KD and CH potentials.

The only available experimental differential cross section data for the transfer to the ^{21}O ground state $\frac{5}{2}^+$ and excited state $\frac{1}{2}^+$ at 10.5 MeV/nucleon beam energy are quite well described by our calculations including the core excitation. Some sensitivity to the underlying potential was observed, but the core-excitation effects turn out to be almost independent of it. The precise value of the quadrupole vibrational coupling β_2 also turns out to be irrelevant provided that spectroscopic factors are fixed that we take from shell-model calculations. At this lowest considered energy we found that the core-excitation effect can be approximated to a good accuracy (6% for the $\frac{1}{2}^+$ state and even better for the $\frac{5}{2}^+$ state) by a simple reduction of the single-particle cross section according to the respective SF. Thus, the extraction of the SF through the ratio of experimental data and single-particle cross section as performed in Ref. [16] is a reasonable procedure. Nevertheless, our prediction for a slightly stronger reduction of the $\frac{1}{2}^+$ cross section leads to an even better agreement between the shell model SF and experimental data.

The situation changes dramatically at higher energy where the core-excitation effects are much more compli-

cated than just a reduction of the cross section according to the respective SF. Thus, in this regime one really needs to perform full calculations with the core excitation and should not rely on a single-particle cross section to extract the SF. For example, we found that at 31.5 MeV/nucleon beam energy the SF extracted in this naive way would be about 70% too small for the $\frac{1}{2}^+$ state but 80% too large for the $\frac{5}{2}^+$ state. This also demonstrates that core excitation acts very differently in the S and D -wave neutron states. In the S -wave case the results are qualitatively consistent with previous findings for reactions involving the $^{11}\text{Be}(\frac{1}{2}^+)$ but based on the rotational model.

Taking into account also the study of the $^{21}\text{O}^*(p,d)^{20}\text{O}(2^+)$ reaction, we are able to make an important conclusion on a systematic effect of the quadrupole core excitation at higher energies: it substantially suppresses reactions with $\ell = 0$ transfer but enhances those with $\ell = 2$. The shape of the angular distribution of the differential cross section is changed in both cases. Of course, the quantitative size of these effects depends on the collision, binding, and excitation energies. Furthermore, the core-excitation effect is a result of a complicated interplay between its contributions of the two- and three-body nature; including only the two-body effect through the modification of the potential is computationally simpler but not justified.

This work was supported by Lietuvos Mokslo Taryba (Research Council of Lithuania) under Contract No. MIP-094/2015. A.D. acknowledges also the hospitality of the Ruhr-Universität Bochum where a part of this work was performed.

References

- [1] T. Tamura, *Rev. Mod. Phys.* 37 (1965) 679.
- [2] R. J. Ascutto, N. K. Glendenning, *Phys. Rev.* 181 (1969) 1396.
- [3] N. K. Glendenning, R. S. Mackintosh, *Nucl. Phys. A* 168 (1971) 575.
- [4] R. S. Mackintosh, *Nucl. Phys. A* 170 (1971) 353.
- [5] R. Ascutto, C. King, L. McVay, B. Sorensen, *Nucl. Phys. A* 226 (1974) 454.
- [6] A. M. Moro, R. Crespo, *Phys. Rev. C* 85 (2012) 054613.
- [7] A. Moro, J. A. Lay, *Phys. Rev. Lett.* 109 (2012) 232502.
- [8] N. C. Summers, F. M. Nunes, *Phys. Rev. C* 76 (2007) 014611.
- [9] R. de Diego, J. M. Arias, J. A. Lay, A. M. Moro, *Phys. Rev. C* 89 (2014) 064609.
- [10] L. D. Faddeev, *Zh. Eksp. Teor. Fiz.* 39 (1960) 1459 [*Sov. Phys. JETP* 12 (1961) 1014].
- [11] E. O. Alt, P. Grassberger, W. Sandhas, *Nucl. Phys. B2* (1967) 167.
- [12] A. Deltuva, *Phys. Rev. C* 88 (2013) 011601(R).
- [13] A. Deltuva, *Phys. Rev. C* 91 (2015) 024607.
- [14] A. Deltuva, A. Ross, E. Norvaišas, F. M. Nunes, *Phys. Rev. C* 94 (2016) 044613.
- [15] R. C. Johnson, P. J. R. Soper, *Phys. Rev. C* 1 (1970) 976.
- [16] B. Fernández-Domínguez, *et al.*, *Phys. Rev. C* 84 (2011) 011301.
- [17] C. Hajduk, P. U. Sauer, W. Struerve, *Nucl. Phys. A* 405 (1983) 581.
- [18] A. Deltuva, R. Machleidt, P. U. Sauer, *Phys. Rev. C* 68 (2003) 024005.

- [19] J. R. Taylor, Nuovo Cimento B 23 (1974) 313, ; M. D. Semon, J. R. Taylor, Nuovo Cimento A 26 (1975) 48.
- [20] E. O. Alt, W. Sandhas, Phys. Rev. C 21 (1980) 1733.
- [21] A. Deltuva, A. C. Fonseca, P. U. Sauer, Phys. Rev. C 71 (2005) 054005.
- [22] J. K. Jewell, *et al.*, Phys. Lett. B 454 (1999) 181.
- [23] E. Khan, *et al.*, Phys. Lett. B 490 (2000) 45.
- [24] F. D. Becchetti Jr., G. W. Greenlees, Phys. Rev. 182 (1969) 1190.
- [25] A. J. Koning, J. P. Delaroche, Nucl. Phys. A713 (2003) 231.
- [26] R. L. Varner, W. J. Thompson, T. L. McAbee, E. J. Ludwig, T. B. Clegg, Phys. Rep. 201 (1991) 57.
- [27] E. K. Warburton, B. A. Brown, Phys. Rev. C 46 (1992) 923.
- [28] Y. Utsuno, T. Otsuka, T. Mizusaki, M. Honma, Phys. Rev. C 60 (1999) 054315.
- [29] K. Amos, L. Canton, G. Pisent, J. Svenne, D. van der Knijff, Nucl. Phys. A 728 (2003) 65.
- [30] R. Machleidt, Phys. Rev. C 63 (2001) 024001.
- [31] R. B. Wiringa, V. G. J. Stoks, R. Schiavilla, Phys. Rev. C 51 (1995) 38.